Journal of Chromatography A, 1217 (2010) 5901–5912

Contents lists available at ScienceDirect

Journal of Chromatography A

journal homepage: www.elsevier.com/locate/chroma

Thermodynamic and kinetic study of chiral separations of coumarin-based anticoagulants on derivatized amylose stationary phase

Kahsay G. Gebreyohannes, Victoria L. McGuffin*

Department of Chemistry, Michigan State University, East Lansing, MI 48824-1322, USA

ARTICLE INFO

Article history:
Received 10 May 2010
Received in revised form 9 July 2010
Accepted 13 July 2010
Available online 22 July 2010

Keywords:
Enantioseparation
Chiralpak IA
Coumarin anticoagulants
Thermodynamic parameters
Kinetic parameters

ABSTRACT

Thermodynamic and kinetic studies are performed on amylose derivatized with tris-(3,5-dimethylphenyl carbamate) stationary phase for the chiral separation of coumarin-based anticoagulants. Polar-organic eluents that contain acetonitrile as bulk solvent with modifiers such as methanol, *i*-butanol, *t*-butanol, and tetrahydrofuran are used in the study. Temperature is varied from 5 to 45 °C at constant pressure of 1500 psi. In general, both retention and enantioselectivity decrease as the temperature increases and as hydrogen bond donating ability of the modifiers increases. The van't Hoff plots are found to show both linear and non-linear behavior. The non-linear plots are believed to be the result of conformational changes in the derivatized amylose phase and are observed around room temperature. The retention behavior in acetonitrile mobile phase provides a linear enthalpy–entropy compensation plot, indicating that all coumarins may have a similar retention mechanism. In contrast, enthalpy–entropy compensation is not observed for warfarin and coumatetralyl enantiomers when separated with different organic modifiers in the mobile phase. The kinetic data indicate that the rate of sorption is always greater than the rate of desorption. An increase in the concentration of alcohol modifiers causes an increase in the desorption rate constant. In contrast, an increase in the concentration of tetrahydrofuran causes a decrease in the desorption rate constant. This effect is most significant for the second eluted enantiomer of coumatetralyl, for which the desorption rate is 36 times slower than the first eluted enantiomer.

1. Introduction

Chiral stationary phases based on derivatized polysaccharides have been widely used for the direct separation of enantiomers in both analytical and preparative applications. These derivatives include the tris-(3,5-dimethylphenyl carbamate) of amylose, tris-(3,5-dimethylphenyl carbamate) of cellulose, tris-(S-α-methylbenzyl carbamate) of amylose, and tris-(*p*-methylbenzoate) of cellulose [1–3]. Among these phases, amylose derivatized with tris-(3,5-dimethylphenyl carbamate) is the most successful for chiral separations in liquid chromatography [4–9]. This phase has five chiral centers per glucose moiety, together with hydrogen bonding and π-electron donor sites. It is commercially available as coated (Chiralpak AD) and chemically immobilized (Chiralpak IA) forms. Unlike the coated form, the immobilized form has greater solvent versatility [10] and temperature stability.

Due to the complex structure of polysaccharide phases, the exact mechanism of chiral separations is not completely understood. These phases have multiple types of interaction sites, both chiral and achiral, with different affinities for the enantiomers. The so-called "multi-site" or "site-selective" thermodynamic and kinetic approaches [11,12] have had limited utility for the polysaccharide phases. As a consequence, it is most common and most effective to treat these stationary phases as a single, heterogenous surface. One way to elucidate the complex retention mechanism is to examine the temperature dependence of retention and enantioselectivity. Insight can then be obtained from van't Hoff plots, i.e., the natural logarithm of the retention factor or enantioselectivity versus the reciprocal of absolute temperature [13]. Linear [14–19] and non-linear [18,20–22] van't Hoff plots have been observed for chiral separations using polysaccharide stationary phases. Linear van't Hoff plots indicate that the separation mechanism is unchanged in the temperature range studied (i.e., ΔH and ΔS values are constant with temperature). Non-linear van't Hoff plots are usually attributed to a change in the retention mechanism as a result of either a change in the conformation of the stationary phase or multiple types of binding sites [13]. Temperature-induced conformational changes of polysaccharide phases have been reported by Wang et al. [18,22]. The van't Hoff plots obtained for the retention factor and enantioselectivity of dihydropyrimidinone (DHP) acid when heating the amylose column from 5 to 50 °C were not superimposable on those obtained upon cooling from 50 to 5 °C. The authors concluded that the

* Corresponding author at: Department of Chemistry, Michigan State University, East Lansing, MI 48824-1322, USA. Tel.: +1 517 355 9715; fax: +1 517 353 1793.
E-mail address: mcguffin@msu.edu (V.L. McGuffin).

0021-9673/$ – see front matter © 2010 Elsevier B.V. All rights reserved.
doi:10.1016/j.chroma.2010.07.043

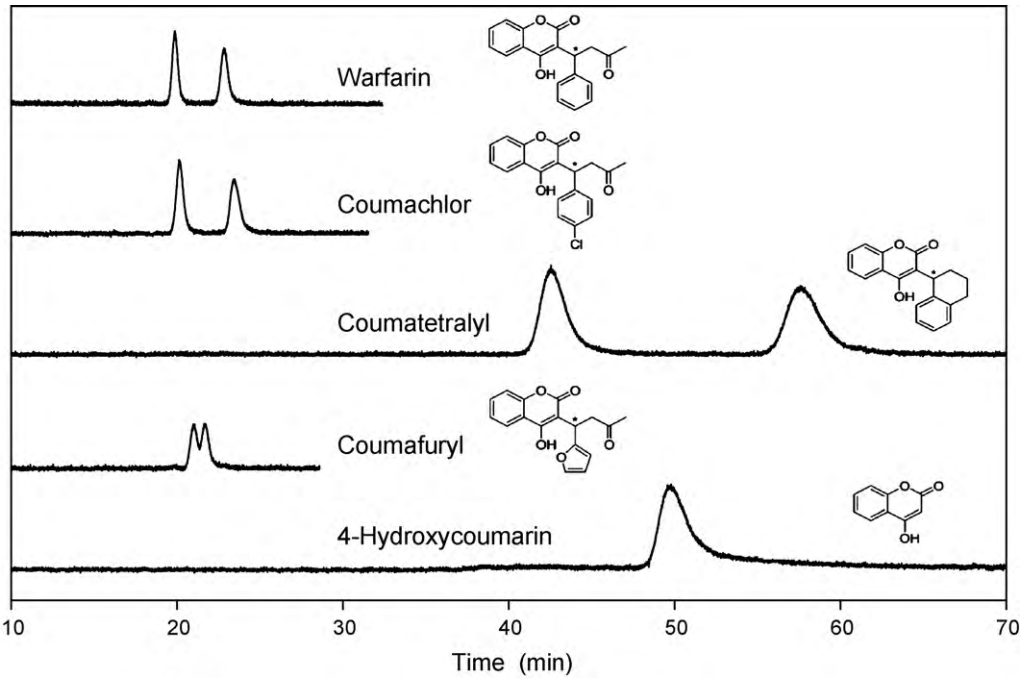

Fig. 1. Chromatograms and structures of coumarin-based anticoagulants. Column: Chiralpak IA; mobile phase: acetonitrile with 0.1% acetic acid and 0.2% triethylamine additives; temperature: 20 °C; flow rate: 1 μL/min.

thermally induced, path-dependent behavior resulted from slow equilibration of the amylose phase. Such conformational changes in the stationary phase can affect sorption and desorption rates. Rizzi [23] reported two types of binding sites for microcrystalline cellulose triacetate that differ in their rates of sorption and desorption. According to his model, one type of sorption site is easily accessible ("quick" site), while the other site is sterically hindered ("slow" site), and they differ in their types of interaction with analytes.

The thermodynamic and kinetic properties of solute transfer can also be affected by the mobile phase composition. The solvent may cause changes in the availability and accessibility of the sorption sites by modifying the size, crystallinity, and shape of chiral cavities [23,24]. Wang et al. [25] utilized solid-state NMR to identify structural changes in the tris-(3,5-dimethylphenyl carbamate) amylose phase as a function of mobile phase composition. *i*-Propanol modifier displayed more efficient displacement of incorporated hexane and formed relatively more ordered solvent complexes compared to ethanol. Kasat et al. [26] used infrared spectroscopy, X-ray diffraction, and solid-state NMR to elucidate the role of solvent in modifying the structure of the amylose phase. The authors concluded that the type of solvent determines the extent of changes of the crystallinity of the polymer. These changes are more substantial for polar and hydrogen bonded solvents such as alcohols and less for non-polar solvents such as hexane.

In this study, we have investigated the effect of both temperature and mobile phase modifiers on the separation of coumarin solutes on tris-(3,5-dimethylphenyl carbamate) amylose in the polar-organic mode. The polar-organic eluents usually consist of methanol, ethanol, acetonitrile, or their combinations. This mode provides an alternative chiral recognition mechanism by separating enantiomers that cannot be separated by either normal-phase or reversed-phase modes [27]. Easy evaporation of the solvents used in this mode is especially attractive for preparative-scale applications [28]. This thermodynamic and kinetic study is intended to provide a deeper understanding of this stationary phase and its chiral recognition mechanism.

2. Materials and methods

2.1. Chemicals

Coumarin-based anticoagulants, consisting of warfarin, coumachlor, coumafuryl, and coumatetralyl, are selected as model solutes for this study. An achiral solute, 4-hydroxycoumarin, that shares a common structural backbone with the chiral coumarins is also employed. The structures of these solutes are shown as insets in Fig. 1. The solutes are obtained from Sigma–Aldrich as solids and are dissolved in high-purity acetonitrile (Burdick and Jackson, Honeywell) to yield standard solutions at 10^{-3} M concentration. The polar-organic mobile phases consist of bulk acetonitrile together with organic modifiers and acid/base additives. High-purity methanol (Burdick and Jackson, Honeywell), *i*-butanol, *t*-butanol (ACS reagent grade, Columbus Chemical Industries, Inc.), and tetrahydrofuran (reagent grade, Jade Scientific) are used as modifiers. Acetic acid and triethylamine (Sigma–Aldrich) are used as additives at 0.1% (0.18 M) and 0.2% (0.14 M) concentration, respectively, for all mobile phase compositions [29].

2.2. Instrumental system

For this study, liquid chromatography is performed with an optically transparent, fused-silica capillary column (200 μm inner diameter (i.d.), 110 cm length, Polymicro Technologies). Before the column is packed, a detection window is created ~84 cm from the inlet by removing the polyimide coating. The column is terminated using a quartz wool frit. The stationary phase, which consists of tris-(3,5-dimethylphenyl carbamate) amylose immobilized on 5 μm silica particles (Chiralpak IA, Chiral Technologies), is then packed using the slurry method [30]. This method provides a column with uniform packing density along the length and diameter. It involves selection of a solvent that will result in slow settling and minimal aggregation of particles of the stationary phase. Among the solvents tested (methanol, acetonitrile, acetone, ethyl acetate, tetrahydrofuran, and hexane), methanol is found to be the best for packing the Chiralpak IA stationary phase. The resulting column has a plate

height of 16 μm and a reduced plate height of 3.2 determined with a neutral solute (pyrene).

The mobile phase is delivered by a single-piston reciprocating pump (Model 114M, Beckman Instruments), operated in the constant pressure mode at 1500 psi. After injection (Model EC14W1, Valco Instruments), the samples are split between the column and a fused-silica capillary (50 μm i.d., 6 m length, Polymicro Technologies) to prevent excessive broadening and overload of the stationary phase. The injection volume is approximately 15 nL. To vary the temperature between 5 and 45 °C, the column, injector, and splitter are housed within a cryogenic oven (Model 3300, Varian Associates). Column equilibration is ensured by alternately cycling the temperature between 5 and 50 °C. At each temperature, the column is equilibrated for an hour and the most retained solute, coumatetralyl, is then injected in triplicate. The calculated retention factors (±0.9% relative standard deviation) and enantioselectivities (±0.6% relative standard deviation) are found to be constant for each temperature and for each cycle.

Laser-induced fluorescence is used for on-column detection. A helium–cadmium laser (Model 3074-20M, Melles Griot) provides excitation at 325 nm. The laser is focused onto a UV-grade optical fiber (100 μm, Polymicro Technologies) and is transmitted to the column window where the polyimide coating has been removed. The fluorescence power is collected orthogonally by a large diameter optical fiber (500 μm, Polymicro Technologies), isolated at 420 nm by an interference filter (S10-410-F, Corion), and transmitted to a photomultiplier tube (Model R760, Hamamatsu). The resulting photocurrent is amplified, converted to the digital domain (Model PCIMIO-16XE-50, National Instruments), and stored by a user-defined program (Labview, v5.1, National Instruments).

2.3. Data analysis

To extract thermodynamic and kinetic information, statistical moments are used because they make no assumptions about the shape of the solute zone profiles or the mechanism of retention. The individual zone profiles are extracted from the chromatogram and fit using non-linear regression (Tablecurve, v2.02, SYSTAT Software, Inc.), so that the statistical moments can be determined without contributions from noise. Gaussian and asymmetric double sigmoidal (ADS) functions are used for fitting, since these two functions are found to provide good quality of fit ($r^2 > 0.998$) and random residuals. The Gaussian function is

$$C(t) = a_0 \exp\left[-0.5\left(\frac{t-a_1}{a_2}\right)^2\right] \quad (1)$$

where a_0 is the amplitude, a_1 is the peak center, and a_2 is the peak width. Similarly, the ADS function is

$$C(t) = \left[\frac{a_0}{1+\exp\left[-\left(\frac{t-a_1+(a_2/2)}{a_3}\right)\right]}\right] \times \left[1-\frac{1}{1+\exp\left[-\left(\frac{t-a_1-(a_2/2)}{a_4}\right)\right]}\right] \quad (2)$$

where a_0 is the amplitude, a_1 is the peak center, and a_2, a_3, and a_4 are peak widths. Using the fitting parameters from both functions, the peaks are regenerated in a spreadsheet program (Excel, v2003, Microsoft Corporation). The first (M_1) and second (M_2) statistical moments are calculated from the zone profiles as

$$M_1 = \frac{\int C(t)t\,dt}{\int C(t)\,dt} \quad (3)$$

$$M_2 = \frac{\int C(t)(t-M_1)^2\,dt}{\int C(t)\,dt} \quad (4)$$

where $C(t)$ is the concentration as a function of time. For this study, the integration limits are taken at 0.1% of the maximum peak height. This integration limit provides minimum error in the determination of statistical moments [31].

The first moment represents the mean retention time (t_r) and is used to determine the retention factor. Since the stationary phase has multiple interaction sites with analytes, it is difficult to find a non-retained marker (t_0) having no interaction with the stationary phase. Based on previous reports in the literature, nitromethane [32], 1,3,5-tri-(*t*-butyl)benzene [10], 4-bromomethyl-7-methoxycoumarin [33], and pyrene are tested as non-retained solutes. However, they are more retained than the least retained solute (warfarin) or are not detected. Consequently, the t_0 marker is determined as follows. At each temperature and mobile phase composition, flow rates are carefully measured before sample injection and after sample elution. The least retained solute, warfarin, is separated in the presence of only 0.2% triethylamine additive in the acetonitrile mobile phase. In the absence of acetic acid, the warfarin peak is found to elute very early, and the enantiomers are unresolved and fronting compared to those observed in the presence of both additives [29]. Values of t_0 are then taken from the first rising edge of this peak, at each temperature and flow rate, for each mobile phase composition. Then, graphs of t_0 and inverse flow rate ($1/F$) versus inverse temperature ($1/T$) are constructed. These plots are found to be linear ($r^2 > 0.999$). Consequently, the slope and intercept of a graph of t_0 versus $1/F$ ($t_0 = 655.68/F - 73.49$; $r^2 = 0.999$) are used to predict t_0 values for each solute injection depending on the measured flow rate. The retention factor (k) is then calculated as

$$k = \frac{(M_1 - t_0)}{t_0} \quad (5)$$

Enantioselectivity (α) is calculated as

$$\alpha = \frac{k_2}{k_1} \quad (6)$$

where k_1 and k_2 are the retention factors for the first and second eluted enantiomer, respectively. Retention factors and selectivities calculated in this manner represent the average values for all interaction sites, both chiral and achiral, on the stationary phase.

The second moment represents the peak variance and is used to determine kinetic rate constants. The second moment is related to the plate height (H) by [34]

$$H = \frac{M_2 L}{M_1^2} \quad (7)$$

where L is the column length. From Giddings generalized non-equilibrium theory [35], the mass transfer term for slow kinetics (C_s) is given by

$$C_s = \frac{2k}{(1+k)^2 k_{ms}} \quad (8)$$

Thus, the desorption rate constant (k_{ms}) can be determined as

$$k_{ms} = \frac{2ku}{(1+k)^2 \Delta H} \quad (9)$$

where u is the linear velocity and ΔH is the corrected plate height, which represents slow mass transfer in the stationary phase (C_s). The sorption rate constant (k_{sm}) can then be determined from the expression for k, which relates the thermodynamic and kinetic terms

$$k = \frac{k_{sm}}{k_{ms}} \quad (10)$$

Table 1
Retention factor (k) and enantioselectivity (α) for coumarin-based solutes in acetonitrile mobile phase at 20 °C.

Solute	k_1[a]	k_2[a]	α
Warfarin	0.99	1.29	1.30
Coumachlor	1.02	1.35	1.35
Coumafuryl	1.10	1.18	1.07
Coumatetralyl	3.29	4.82	1.46
4-Hydroxycoumarin	4.13	N/A[b]	N/A

[a] Subscripts denote the first (1) and second (2) eluted enantiomers.
[b] Not applicable (N/A).

$$k_{sm} = \frac{2k^2u}{(1+k)^2\Delta H} \quad (11)$$

The corrected plate height is calculated as

$$\Delta H = H - A - \frac{B}{u} - C_m u \quad (12)$$

where H is the total plate height determined for each solute from Eq. (7). A, B, and C_m are the individual column contributions to zone broadening from multiple paths, diffusion in the mobile and stationary phases, and resistance to mass transfer in the mobile phase, respectively [36]. In this study, the column contributions are determined by injection of 10^{-4} M pyrene. The use of a non-polar aromatic hydrocarbon for plate height determination on cellulose triacetate stationary phase was demonstrated previously by Rizzi [23]. These compounds, regardless of their size, always showed low plate height values since they were mainly adsorbed onto sites with faster kinetics. In the present study, the average plate height for pyrene is found to be 16 ± 0.4 μm over the temperature range of 5–45 °C. This relatively constant value with temperature is expected when the multiple path (A) contribution predominates, as is common for packed columns in liquid chromatography [37]. This value is then subtracted from the total plate height measured for each solute, according to Eq. (12). This assumes that all broadening due to axial dispersion and fast mobile phase kinetics is removed, leaving only the slow kinetic contribution from the stationary phase. The corrected plate height is then used to calculate the rate constants using Eqs. (10) and (11). Rate constants calculated in this manner represent the average values for all interaction sites, both chiral and achiral, on the stationary phase.

3. Results and discussion

3.1. Thermodynamic effects

The separation of the chiral coumarins (warfarin, coumachlor, coumafuryl, and coumatetralyl) and an achiral coumarin (4-hydroxycoumarin) on Chiralpak IA using acetonitrile mobile phase is shown in Fig. 1. Values of the retention factor and enantioselectivity at 20 °C are listed in Table 1. Comparison of the retention behavior of the first eluted enantiomer indicates that warfarin, coumachlor, and coumafuryl have comparable retention factors, with warfarin being the least retained. The achiral solute, 4-hydroxycoumarin, is the most retained. With no side chain at the 3-position, 4-hydroxycoumarin can have simultaneous interactions of the hydroxyl and carbonyl groups with the carbamate group and/or residual hydroxyl or silanol groups of the stationary phase [32]. Nevertheless, 4-hydroxycoumarin is less retained than the second enantiomer of coumatetralyl. This may be a result of fewer interaction sites for 4-hydroxycoumarin in the derivatized stationary phase or, alternatively, because the chiral sites are conformationally well suited for the second eluted enantiomer of coumatetralyl.

The chiral solutes, with the exception of coumafuryl, have excellent enantioseparation in the stationary phase. In coumafuryl, the hydroxyl side chain may form intramolecular hydrogen bonds with the oxygen atom of the furan ring, resulting in the loss of binding sites that may contribute to chiral recognition.

Table 2
Solvatochromic properties of modifiers used in the study [38].

Modifier	α[a]	β[a]
Methanol (MeOH)	0.93	(0.62)
i-Butanol (*i*-BuOH)	N/A[b]	N/A
t-Butanol (*t*-BuOH)	0.68	(1.01)
Tetrahydrofuran (THF)	0.00	(0.55)[c]

[a] Hydrogen bond donating ability (α); hydrogen bond accepting ability (β).
[b] Not available (N/A).
[c] Data in parentheses are relatively less certain.

3.1.1. Effect of modifier type and concentration on retention and enantioselectivity

To investigate the effect of organic modifiers on the thermodynamics of the separation on Chiralpak IA, warfarin and coumatetralyl are chosen as model solutes. The modifiers used for this study are alcohols such as methanol (MeOH), *i*-butanol (*i*-BuOH), *t*-butanol (*t*-BuOH), and tetrahydrofuran (THF). These modifiers have differences in their hydrogen bond donating/accepting abilities (Table 2 [38]). Alcohols can act as both proton donors and acceptors, while tetrahydrofuran is a proton acceptor. The modifiers also have differences in molecular size and shape. Methanol is smaller in size, while *i*-BuOH and *t*-BuOH are branched and relatively bulky. THF has size comparable to that of *t*-BuOH. Kasat et al. [26] have reported that the size of the cavity formed by intramolecular hydrogen bonds between C=O and N–H groups of the derivatized amylose phase increases as the molecular size of the modifiers increases. Branched alcohols cause twisting of the α-(1,4)-glycosidic linkage of the amylose helix, as evidenced by the reduction in the chemical shift of C_1 and C_4 sites using ^{13}C cross-polarization and magic angle spinning (CP/MAS) solid-state NMR [39,40].

The retention and enantioselectivity of warfarin enantiomers in varying modifier concentrations are summarized in Table 3 and are

Table 3
Effect of organic modifier type and concentration on retention factor (k) and enantioselectivity (α) for warfarin and coumatetralyl enantiomers at 20 °C.

Solute	Modifier	5%			10%		
		k_1[a]	k_2[a]	α	k_1	k_2	α
Warfarin	MeOH	0.97	1.10	1.13	0.96	1.03	1.07
	i-BuOH	0.93	1.10	1.18	0.89	0.98	1.10
	t-BuOH	1.06	1.28	1.21	0.89	1.02	1.14
	THF	1.04	1.33	1.28	0.99	1.31	1.32
Coumatetralyl	MeOH	1.90	2.35	1.24	1.41	1.61	1.14
	i-BuOH	2.03	2.81	1.38	1.44	1.82	1.26
	t-BuOH	2.93	4.60	1.57	1.47	2.06	1.40
	THF	3.08	4.83	1.57	2.31	4.31	1.87

[a] Subscripts denote the first (1) and second (2) eluted enantiomers.

compared to values in the absence of modifier in Table 1. At 5% modifier concentration, the retention factors of warfarin enantiomers decrease in MeOH and *i*-BuOH, but remain constant or increase in *t*-BuOH and THF. In contrast, the enantioselectivity of warfarin is found to decrease as the proton donating ability of the alcohol modifiers increases. At 10% modifier concentration, both the retention factor and enantioselectivity of warfarin are found to further decrease in the alcohol modifiers. In THF, retention factors for the warfarin enantiomers are not significantly affected and, as a result, the enantioselectivity remains almost constant.

The retention and enantioselectivity of coumatetralyl enantiomers in varying modifier concentrations are summarized in Table 3 and are compared to values in the absence of modifier in Table 1. At 5% modifier concentration, the retention factor of the first eluted enantiomer decreases in all modifiers. For the second eluted enantiomer, retention remains constant in THF, but decreases in the other modifiers. Accordingly, the enantioselectivity of coumatetralyl decreases in MeOH and *i*-BuOH, but increases in *t*-BuOH and THF by about 7.5%. Despite the different retention behavior of the two enantiomers in *t*-BuOH and THF, the magnitude of the enantioselectivity in both modifiers is identical. At 10% modifier concentration, the retention factor and enantioselectivity of coumatetralyl enantiomers are found to decrease substantially as the proton donating ability of the alcohol modifiers increases. THF causes a decrease in the retention factors of both enantiomers by about 29% and 12%, respectively. However, the enantioselectivity is found to increase substantially by about 28%. This suggests that the second eluted enantiomer of coumatetralyl may have a better conformational fit in the chiral cavity of the stationary phase than the first eluted enantiomer.

3.1.2. Effect of temperature on retention and enantioselectivity

To investigate the effect of temperature on retention and enantioselectivity in acetonitrile mobile phase, van't Hoff plots are obtained for the temperature range of 5–45 °C. The dependence of retention factor on temperature is given by

$$\ln k = \frac{-\Delta G}{RT} - \ln \beta = \frac{-\Delta H}{RT} + \frac{\Delta S}{R} - \ln \beta \quad (13)$$

where ΔG, ΔH, and ΔS represent the changes in molar Gibbs free energy, enthalpy, and entropy, respectively, R is the gas constant, T is the absolute temperature, and β is the volumetric ratio of the mobile and stationary phases [41]. Eq. (13) indicates that a graph of the natural logarithm of the retention factor versus the inverse of the absolute temperature should be linear with a slope of $(-\Delta H/R)$ and an intercept of $(\Delta S/R - \ln \beta)$, if ΔH, ΔS, and β are independent of temperature. The dependence of enantioselectivity on temperature is given by

$$\ln \alpha = \frac{-\Delta\Delta G}{RT} = \frac{-\Delta\Delta H}{RT} + \frac{\Delta\Delta S}{R} \quad (14)$$

where $\Delta\Delta G$, $\Delta\Delta H$, and $\Delta\Delta S$ represent the differential changes in molar Gibbs free energy, enthalpy, and entropy, respectively, between enantiomers according to Eq. (6) [41,42]. A graph of the natural logarithm of enantioselectivity versus inverse temperature will be linear with a slope of $(-\Delta\Delta H/R)$ and an intercept of $(\Delta\Delta S/R)$, if $\Delta\Delta H$ and $\Delta\Delta S$ are independent of temperature. In chiral separations, only stereoselective interactions with the chiral selector lead to a difference in the retention of enantiomeric pairs.

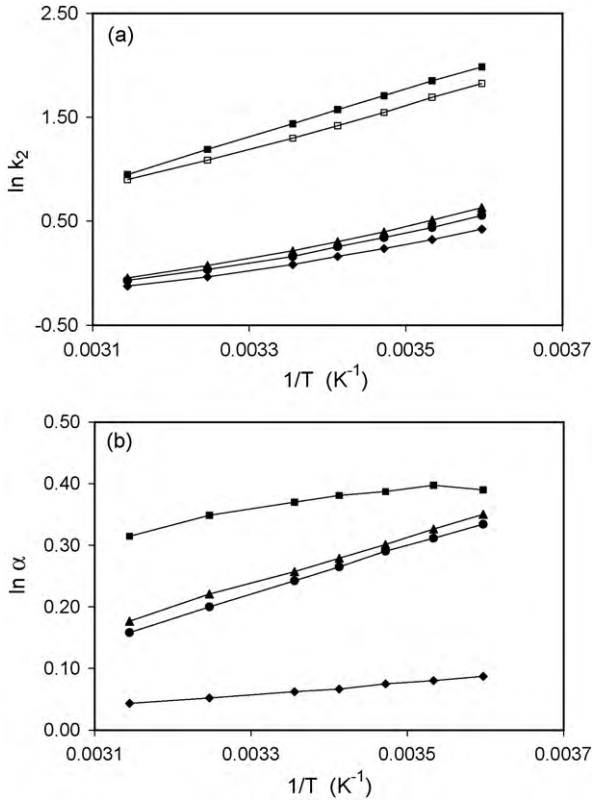

Fig. 2. The van't Hoff plots for all coumarin enantiomers: (a) natural logarithm of the retention factor of the second eluted enantiomer (k_2) versus inverse temperature ($1/T$), (b) natural logarithm of enantioselectivity (α) versus $1/T$. Warfarin (●), coumachlor (▲), coumafuryl (♦), coumatetralyl (■), and 4-hydroxycoumarin (□). Other experimental conditions as given in Fig. 1.

The van't Hoff plots for the retention factor ($\ln k$ versus $1/T$) of the coumarins in acetonitrile mobile phase are shown in Fig. 2a. As can be seen, the plots are linear with correlation coefficients (r^2) ranging from 0.989 to 0.999. Similarly, the van't Hoff plots for the enantioselectivity ($\ln \alpha$ versus $1/T$) of warfarin, coumachlor, and coumafuryl are also linear (Fig. 2b). However, this plot is found to be non-linear ($r^2 = 0.897$) for coumatetralyl, suggesting that the retention mechanism is not independent of temperature in the range investigated.

The thermodynamic parameters obtained from the van't Hoff plots in acetonitrile mobile phase are summarized in Table 4. The estimated values for ΔH and ΔS for all coumarins are found to

Table 4
Thermodynamic parameters for coumarin-based solutes in acetonitrile mobile phase.

Solute	ΔH_1 [a,b] (kJ/mol)	ΔH_2 [a,b] (kJ/mol)	$\Delta\Delta H$ [c] (kJ/mol)	$T\Delta\Delta S$ [c] (kJ/mol)	$\Delta\Delta G$ (kJ/mol)
Warfarin	−8.2 ± 0.5	−11.4 ± 0.5	−3.26 ± 0.04	−2.59 ± 0.04	−0.63 ± 0.04
Coumachlor	−9.2 ± 0.5	−12.3 ± 0.5	−3.13 ± 0.04	−2.47 ± 0.04	−0.67 ± 0.04
Coumafuryl	−9.3 ± 0.4	−10.1 ± 0.5	−0.79 ± 0.04	−0.63 ± 0.04	−0.17 ± 0.04
Coumatetralyl	−17.6 ± 0.1	−19.1 ± 0.1	−1.4 ± 0.2	−0.06 ± 0.02	−1.3 ± 0.2
4-Hydroxycoumarin	−17.0 ± 0.3	N/A[d]	N/A	N/A	N/A

[a] Subscripts denote the first (1) and second (2) eluted enantiomers.
[b] Calculated from the slope of Eq. (13).
[c] Calculated from the slope and intercept of Eq. (14) at T_{hm} (294.6 K, 21.6 °C).
[d] Not applicable (N/A).

be negative. These values indicate that solute transfer from the mobile to stationary phase is enthalpically favorable but entropically unfavorable. The change in molar enthalpy is found to be comparable for the first eluted enantiomer of coumachlor, coumafuryl, and warfarin. In contrast, the values for coumatetralyl and 4-hydroxycoumarin are almost twice those for the other coumarins. The enthalpy change is related to the strength of interactions between the enantiomers and the mobile and stationary phases. In the mobile phase, both enantiomers are solvated identically and, hence, have equal molar enthalpy. In the stationary phase, the enthalpy arises mainly from interactions of specific functional groups of the enantiomer and stationary phase, together with contributions from dispersion and other weak forces. Enantiomeric pairs may have different values for ΔH due to the different orientation of their functional groups as well as their different structural compatibility with the chiral selective sites.

The differential changes in molar enthalpy ($\Delta\Delta H$), entropy ($\Delta\Delta S$), and Gibbs free energy ($\Delta\Delta G$) in acetonitrile mobile phase are also compared in Table 4. The magnitude of the differential change in free energy of the enantiomeric pairs represents the extent of enantioselectivity (Eq. (14)). As can be seen from Table 4, warfarin and coumachlor have comparable differential enthalpic and entropic contributions to their differential free energy. As a result, their chiral selectivities are comparable in magnitude (Table 1). Coumafuryl has the least negative value for $\Delta\Delta H$ and almost equal value for $T\,\Delta\Delta S$, leading to nearly zero $\Delta\Delta G$. In contrast, coumatetralyl has an intermediate contribution to $\Delta\Delta H$, but nearly zero contribution to $T\,\Delta\Delta S$. This solute has a bulky side chain that is conformationally flexible (Fig. 1). Its transfer from the mobile to stationary phase may also be accompanied by the expulsion of a large number of solvent molecules from the stationary phase. This desolvation process and/or conformational flexibility may account for the relatively higher entropic contribution. Accordingly, coumatetralyl has the most negative value of $\Delta\Delta G$ and, hence, the greatest enantioselectivity.

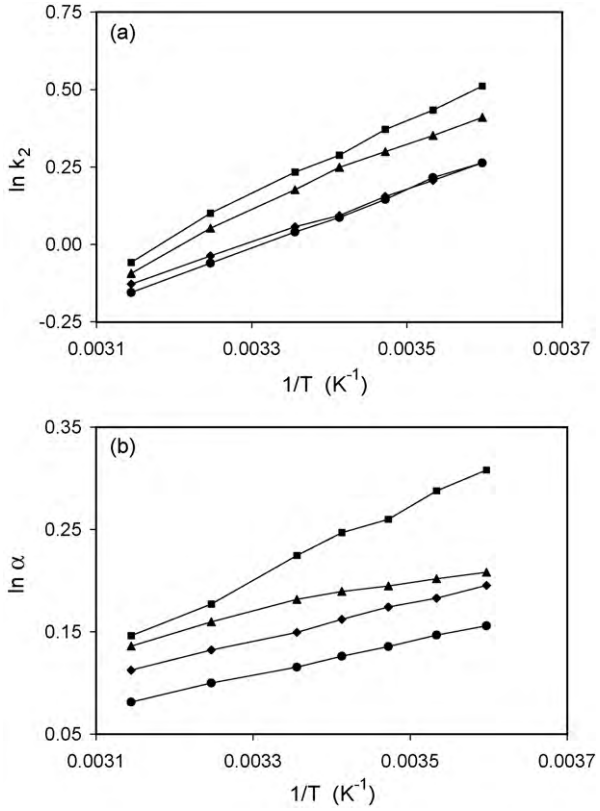

Fig. 3. The van't Hoff plots for warfarin enantiomers: (a) natural logarithm of the retention factor of the second eluted enantiomer (k_2) versus inverse temperature ($1/T$), (b) natural logarithm of enantioselectivity (α) versus $1/T$ in the presence of 5% modifiers. MeOH (●), *i*-BuOH (♦), *t*-BuOH (▲), and THF (■). Other experimental conditions as given in Fig. 1.

3.1.3. *Effect of modifier type and concentration on molar enthalpy, entropy, and Gibbs free energy*

To investigate the effect of organic modifier type and concentration on the thermodynamic parameters of warfarin and coumatetralyl, temperature was varied from 5 to 45 °C. The van't Hoff plots for the retention factor of warfarin enantiomers in the presence of 5% modifiers are shown in Fig. 3a. The plots of $\ln k$ versus $1/T$ obtained in MeOH, *i*-BuOH, *t*-BuOH, and THF are linear ($r^2 = 0.990$–0.999), suggesting that the change in molar enthalpy is independent of temperature in this range. Similarly, the van't Hoff plots for the enantioselectivity of warfarin enantiomers in the presence of 5% modifiers are shown in Fig. 3b. The plots of $\ln \alpha$ versus $1/T$ are found to be linear ($r^2 = 0.996$–0.999) for MeOH, *i*-BuOH, and THF, but non-linear ($r^2 = 0.965$) for *t*-BuOH. It is interesting to note that the slope of the non-linear van't Hoff plot for *t*-BuOH changes around room temperature. In fact, better correlations ($r^2 > 0.999$) are obtained when the plots are taken in the low temperature (5–20 °C) and high temperature (25–45 °C) regions separately.

The van't Hoff plots for the retention factor of coumatetralyl enantiomers with 5% modifiers are shown in Fig. 4a. The plots of $\ln k$ versus $1/T$ are found to be linear ($r^2 = 0.997$–0.999) for MeOH, *i*-BuOH, and THF. For *t*-BuOH, the plot has a slightly different trend for the low temperature (5–20 °C) and high temperature (25–45 °C) regions and, hence, is considered to be non-linear despite an acceptable value of the correlation coefficient ($r^2 = 0.989$). However, the plots are linear ($r^2 = 0.999$) when data for the low and high temperature regions are plotted separately. Similarly, the van't Hoff plots for the enantioselectivity of coumatetralyl enantiomers with 5% modifiers are shown in Fig. 4b. The plots of $\ln \alpha$ versus $1/T$ are found to be linear ($r^2 = 0.996$) in *i*-BuOH, but non-linear in MeOH, *t*-BuOH, and THF modifiers. In the low temperature region, these plots are linear for MeOH and *t*-BuOH, while in the high temperature region, these plots are linear for *t*-BuOH and THF.

Non-linear van't Hoff plots are usually attributed to changes in the retention mechanism or conformation of the stationary phase [13,20–22]. When such changes are observed, the thermodynamic parameters are no longer independent of temperature. For non-linear plots of $\ln \alpha$, $\Delta\Delta H$ values are estimated from the difference between ΔH_2 and ΔH_1 (calculated from the slopes of $\ln k_2$ and $\ln k_1$ versus $1/T$, respectively), and $\Delta\Delta S$ values are estimated from the corresponding difference between the intercepts.

The thermodynamic parameters obtained from the slopes of the van't Hoff plots for the warfarin enantiomers are shown in Table 5. The change in molar enthalpy for both enantiomers becomes more negative (favorable) as the proton donating ability of the alcohol modifiers decreases. However, the differential changes between the enantiomers ($\Delta\Delta H$ and T $\Delta\Delta S$) are statistically comparable in the alcohol modifiers. In THF, the second enantiomer has much stronger interaction with the stationary phase, as evidenced by its more negative change in molar enthalpy. The $\Delta\Delta H$ contribution to the free energy is consequently the most favorable in THF, but the $T\,\Delta\Delta S$ contribution is the least favorable. Despite the unfavorable entropic contribution, THF provides the most favorable $\Delta\Delta G$ and, hence, the greatest enantioselectivity.

The thermodynamic parameters obtained for the coumatetralyl enantiomers are shown in Table 5. Some of the trends observed with the modifiers are similar to those noted above for warfarin. For example, the change in molar enthalpy generally becomes more negative for the coumatetralyl enantiomers as the proton donating ability of the alcohol modifiers decreases. Again, the most nega-

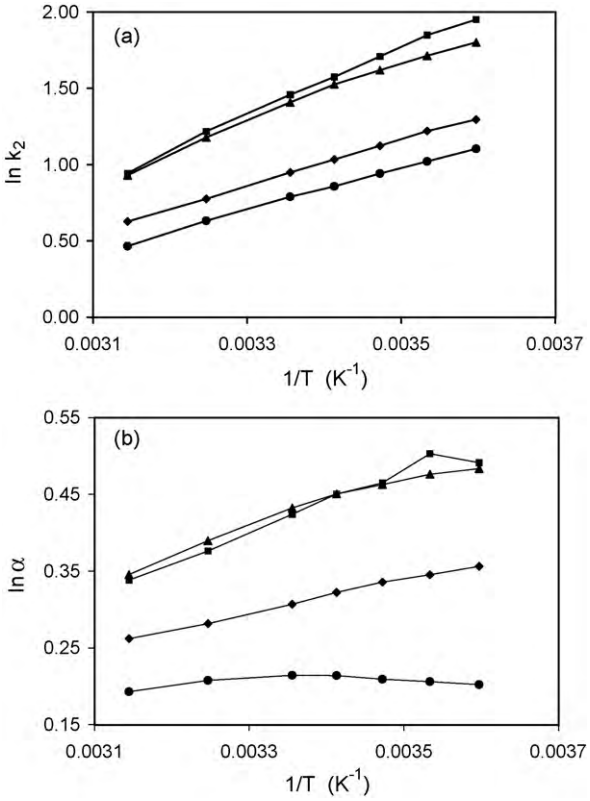

Fig. 4. The van't Hoff plots for coumatetralyl enantiomers: (a) natural logarithm of the retention factor of the second eluted enantiomer (k_2) versus inverse temperature ($1/T$), (b) natural logarithm of enantioselectivity (α) versus $1/T$ in the presence of 5% modifiers. MeOH (●), *i*-BuOH (♦), *t*-BuOH (▲), and THF (■). Other experimental conditions as given in Fig. 1.

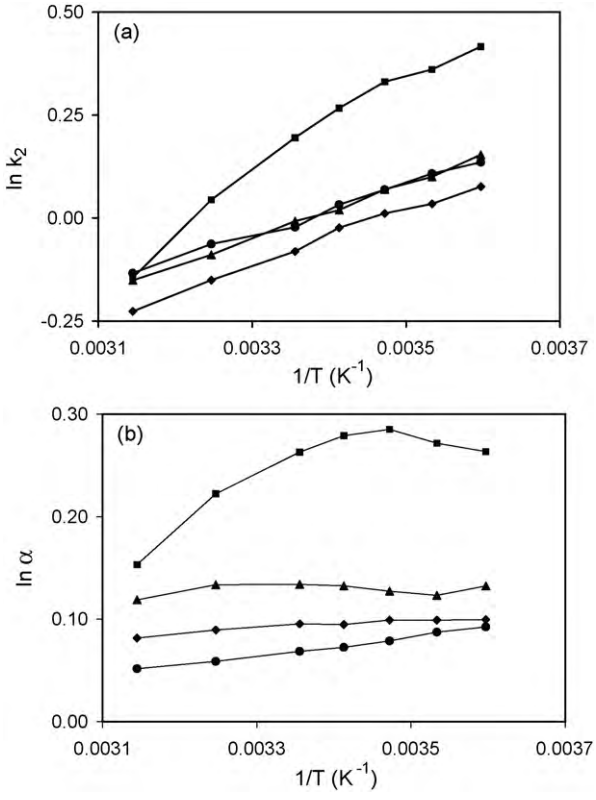

Fig. 5. The van't Hoff plots for warfarin enantiomers: (a) natural logarithm of the retention factor of the second eluted enantiomer (k_2) versus inverse temperature ($1/T$), (b) natural logarithm of enantioselectivity (α) versus $1/T$ in the presence of 10% modifiers. MeOH (●), *i*-BuOH (♦), *t*-BuOH (▲), and THF (■). Other experimental conditions as given in Fig. 1.

tive values are observed in THF, a proton acceptor. However, some trends are notably different. For example, the differential changes in molar enthalpy, entropy, and free energy become increasingly more negative in the alcohols, but are statistically comparable for *t*-BuOH and THF. Although *t*-BuOH and THF have different solvent properties (Table 2), their size is comparable. Hence, the bulky size of these modifiers may play an important role in the separation of coumatetralyl enantiomers [40].

The effect of increasing the modifier concentration to 10% is also investigated. When 10% of each modifier is used, van't Hoff plots for the retention factor of warfarin enantiomers are linear (r^2 = 0.992–0.998) in the alcohol modifiers, but non-linear (r^2 = 0.968) for the more strongly retained enantiomer in THF (Fig. 5a). In contrast, the van't Hoff plots for the enantioselectivity are linear only in MeOH, where the solute is least retained (Fig. 5b). Similarly, the van't Hoff plots for the retention factor of coumatetralyl enantiomers are linear (r^2 = 0.983–0.997) in the alcohol modifiers, but non-linear (r^2 = 0.965) for the more strongly retained enantiomer in THF (Fig. 6a). However, the van't Hoff plots for the enantioselectivity are non-linear in all modifiers (Fig. 6b). Taken together, these results suggest that the stationary phase undergoes a conformational change that occurs between 20 and 25 °C. This change is readily evident at 5% concentration for bulky modifiers such as *t*-BuOH and THF, and for all modifiers at 10% concentration. Because this conformational change occurs around room temperature, it has important implications for the reproducibility of chiral separations that may influence chiral method development and validation.

Table 5
Effect of organic modifier on thermodynamic parameters for warfarin and coumatatralyl enantiomers.

Solute	Modifier (5%)	ΔH_1 [a,b] (kJ/mol)	ΔH_2 [a,b] (kJ/mol)	$\Delta\Delta H$ [c] (kJ/mol)	$T\,\Delta\Delta S$ [c] (kJ/mol)	$\Delta\Delta G$ (kJ/mol)
Warfarin	MeOH	−5.77 ± 0.08	−7.11 ± 0.08	−1.37 ± 0.02	−1.04 ± 0.02	−0.33 ± 0.04
	i-BuOH	−6.2 ± 0.1	−7.7 ± 0.1	−1.50 ± 0.04	−1.13 ± 0.04	−0.38 ± 0.04
	t-BuOH	−7.9 ± 0.3	−9.2 ± 0.4	−1.3 ± 0.5[d]	−0.9 ± 0.1[e]	−0.4 ± 0.5
	THF	−7.2 ± 0.3	−10.3 ± 0.3	−3.01 ± 0.08	−2.42 ± 0.08	−0.58 ± 0.12
Coumatetralyl	MeOH	−11.5 ± 0.1	−11.6 ± 0.2	−0.1 ± 0.2[d]	0.4 ± 0.3[e]	−0.5 ± 0.4
	i-BuOH	−10.7 ± 0.1	−12.4 ± 0.2	−1.80 ± 0.04	−1.00 ± 0.04	−0.75 ± 0.08
	t-BuOH	−13.4 ± 0.5	−16.0 ± 0.7	−2.55 ± 0.21	−1.50 ± 0.21	−1.04 ± 0.29
	THF	−15.4 ± 0.4	−18.5 ± 0.5	−3.09 ± 0.6[d]	−2.01 ± 0.6[e]	−1.08 ± 0.8

[a] Subscripts denote the first (1) and second (2) eluted enantiomers.
[b] Calculated from the slope of Eq. (13).
[c] Calculated from the slope and intercept of Eq. (14) at T_{hm} (294.6 K, 21.6 °C), except as noted.
[d] Non-linear van't Hoff plot, calculated as $\Delta H_2 - \Delta H_1$.
[e] Non-linear van't Hoff plot, calculated as $T\,[(\Delta S/R - \ln\beta)_2 - (\Delta S/R - \ln\beta)_1]$ at T_{hm}.

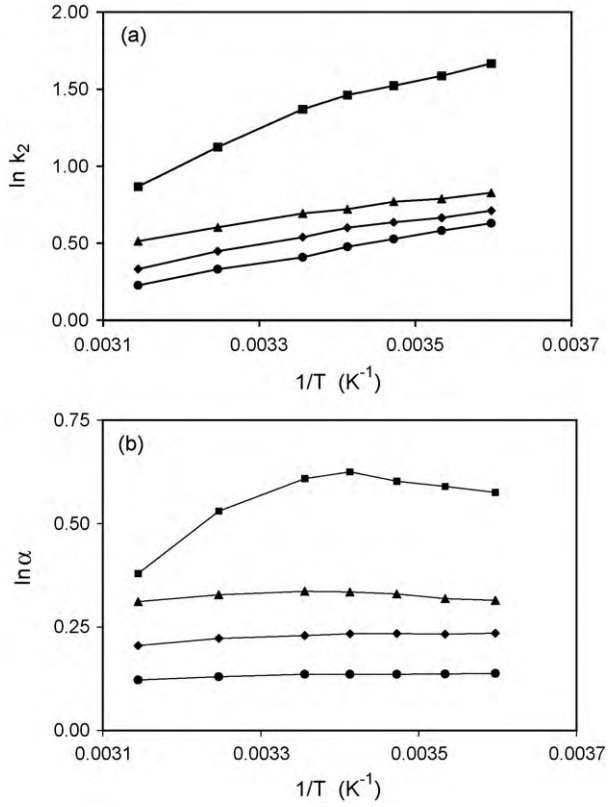

Fig. 6. The van't Hoff plots for coumatetralyl enantiomers: (a) natural logarithm of the retention factor of the second eluted enantiomer (k_2) versus inverse temperature ($1/T$), (b) natural logarithm of enantioselectivity (α) versus $1/T$ in the presence of 10% modifiers. MeOH (●), *i*-BuOH (♦), *t*-BuOH (▲), and THF (■). Other experimental conditions as given in Fig. 1.

3.1.4. Enthalpy–entropy compensation

Enthalpy–entropy compensation (EEC) is often expressed as the linear correlation between the changes in molar enthalpy and entropy for a series of related processes [43–45].

$$\Delta H = T_C \Delta S + \Delta G_{T_C} \quad (15)$$

The compensation temperature (T_C) represents the temperature at which ΔH and ΔS are completely compensated, i.e., the temperature at which there is no enantioselectivity. Krug et al. [43,44] have shown that linear plots of ΔH versus ΔS may arise by propagation of measurement errors, rather than an actual EEC effect. When true EEC exists, however, plots of ΔG versus ΔH must be linear. These linear plots are usually indicative of compensation resulting from similar interactions between the solute and stationary phase [45]. When Eq. (15) is substituted into the definition of Gibbs free energy ($\Delta G = \Delta H - T\Delta S$),

$$\Delta G = \Delta H \left[1 - \frac{T}{T_C}\right] + \frac{T\Delta G_{T_C}}{T_C} \quad (16)$$

Upon substituting Eq. (16) into the relationship between Gibbs free energy and retention factor in Eq. (13),

$$\ln k = \frac{-\Delta H}{R}\left[\frac{1}{T_{hm}} - \frac{1}{T_C}\right] - \frac{\Delta G_{T_C}}{RT_C} + \ln \beta \quad (17)$$

where T_{hm} is the harmonic mean of the absolute temperature ($\langle 1/T\rangle^{-1}$) for the experimental data. Eq. (17) shows that if enthalpy–entropy compensation occurs, a plot of $\ln k$ versus $-\Delta H$ will be linear, and the slope can be used to calculate the compensation temperature. If the compensation temperature is sufficiently higher than the ambient temperature, the separation is usually considered to be enthalpy dominated [46]. In contrast, if the compensation temperature is lower than the ambient temperature, the separation is entropy dominated [46]. At values close to the compensation temperature, enantioseparations cannot be obtained.

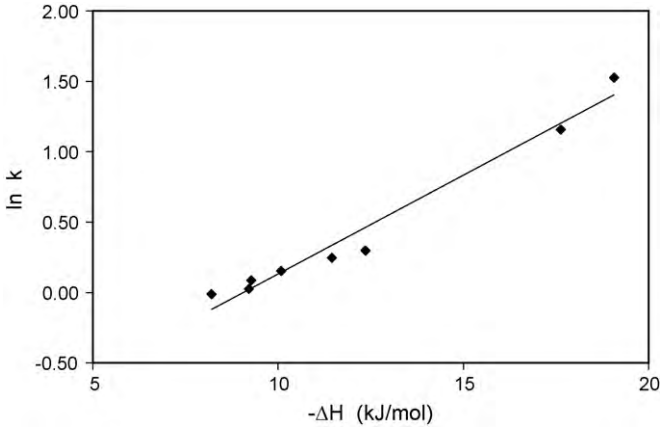

Fig. 7. Enthalpy–entropy compensation plot of the natural logarithm of the retention factor (k) versus change in molar enthalpy ($-\Delta H$) for all coumarin enantiomers in Fig. 1. The equation of the line is $y = 1 \times 10^{-4}\, x - 1.2719$ ($r^2 = 0.971$). Other experimental conditions as given in Fig. 1.

To compare the mechanism of separation of the coumarin solutes on Chiralpak IA, an enthalpy–entropy compensation plot is shown in Fig. 7. The plot of $\ln k$ versus $-\Delta H$ is found to be linear ($r^2 = 0.971$) for all coumarin solutes, however the plot is similarly linear ($r^2 = 0.967$) if the most retained solute, coumatetralyl, is omitted. From the slope of these graphs, the compensation temperature is found to be 176 °C for all solutes and 93 °C for all solutes except coumatetralyl. As both compensation temperatures are clearly above ambient, the separation is enthalpy dominated, which is confirmed by the thermodynamic parameters in Table 4. From these results, warfarin, coumachlor, and coumafuryl appear to have a similar retention mechanism in acetonitrile mobile phase, however coumatetralyl may or may not be different.

The effect of organic modifiers on the separation of warfarin and coumatetralyl enantiomers is demonstrated by the enthalpy–entropy compensation plot in Fig. 8. As can be seen, this graph is non-linear ($r^2 = 0.889$) and no clear compensation is observed for warfarin or coumatetralyl. When the first and second eluted enantiomers are graphed separately, linear plots of $\ln k$

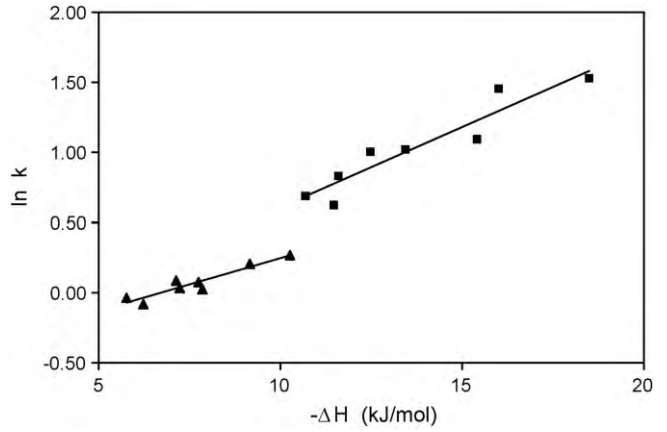

Fig. 8. Enthalpy–entropy compensation plot of the natural logarithm of the retention factor (k) versus change in molar enthalpy ($-\Delta H$) for warfarin (▲) and coumatetralyl enantiomers (■) with 5% of MeOH, *i*-BuOH, *t*-BuOH, and THF. The equation of the lines are: $y = 7 \times 10^{-5}\, x - 0.503$ ($r^2 = 0.889$) for warfarin and $y = 1 \times 10^{-4}\, x - 0.538$ ($r^2 = 0.889$) for coumatetralyl. Other experimental conditions as given in Fig. 1.

Table 6
Sorption (k_{sm}) and desorption (k_{ms}) rate constants for coumarin-based solutes in acetonitrile mobile phase at 10 °C.

Solute	$(k_{sm})_1$ [a] (s^{-1})	$(k_{ms})_1$ (s^{-1})	$(k_{sm})_2$ [a] (s^{-1})	$(k_{ms})_2$ (s^{-1})
Warfarin	3.9	3.4	2.7	1.7
Coumachlor	0.9	0.8	1.6	1.0
Coumafuryl	11.0	8.6	2.5	1.8
Coumatetralyl	1.4	0.3	1.5	0.2
4-Hydroxycoumarin	0.2	0.04	N/A[b]	N/A

[a] Subscripts denote the first (1) and second (2) eluted enantiomers.
[b] Not applicable.

versus $-\Delta H$ are observed only for the second eluted enantiomers. The correlation coefficients for the first and second enantiomers of warfarin are found to be 0.632 and 0.948, respectively. Similarly, the correlation coefficients for the first and second enantiomers of coumatetralyl are 0.863 and 0.939, respectively. The compensation temperatures for the second eluted enantiomers are 77 °C for warfarin and 121 °C for coumatetralyl. These results suggest that the second eluted enantiomer of each solute has a similar retention mechanism in the presence of all organic modifiers (MeOH, *i*-BuOH, *t*-BuOH, THF), whereas the first eluted enantiomer does not. The second eluted enantiomers, necessarily, have greater interaction with the chiral interaction sites. Hence, these modifiers may have similar ability to displace or compete with the solutes at the chiral interaction sites.

3.2. Kinetic effects

The rate at which solute molecules undergo mass transfer between mobile and stationary phases is represented by

$$X_m \underset{k_{ms}}{\overset{k_{sm}}{\rightleftharpoons}} X_s \quad (18)$$

where k_{sm} is the rate constant for transfer from mobile to stationary phase (sorption) and k_{ms} is the rate constant for transfer from stationary to mobile phase (desorption).

The rate constants for sorption and desorption of the coumarin solutes on Chiralpak IA using acetonitrile mobile phase are summarized in Table 6. In general, the rate constant for sorption is greater than that for desorption. For the first eluted enantiomer, the rates of sorption and desorption are fastest for coumafuryl and slowest for coumachlor. For the second eluted enantiomer, the rates are fastest and comparable for coumafuryl and warfarin, but slowest and comparable for coumachlor and coumatetralyl. The rate constants for the achiral solute, 4-hydroxycoumarin, are substantially smaller than those for the chiral coumarins. As noted in Section 3.1 above, 4-hydroxycoumarin does not have a substituent at the 3-position and, hence, can have simultaneous interactions of the hydroxyl and carbonyl groups with the stationary phase. This concerted adsorption may have slower kinetics than the isolated interactions of these groups in the chiral coumarins.

3.2.1. Effect of modifier type and concentration on rate constants

To investigate the effect of organic modifiers on the kinetics of the separation on Chiralpak IA, warfarin and coumatetralyl are chosen as model solutes. The desorption rate constants for warfarin enantiomers in varying modifier concentrations are summarized in Table 7 and are compared to values in the absence of modifier in Table 6. At 5% modifier concentration, the desorption rate constants for both enantiomers increase in all modifiers. This behavior is expected for modifiers that serve as better displacing or competing agents than acetonitrile for sites on the derivatized amylose phase. For the first eluted enantiomer, the desorption rate constant increases slightly in *i*-BuOH and *t*-BuOH and more substantially in MeOH and THF. For the second eluted enantiomer, the desorption rate constant increases significantly in MeOH and *i*-BuOH, but decreases in *t*-BuOH and THF. The rate of mass transfer for the second eluted enantiomer increases with an increase in the proton donating ability of the alcohol modifiers. However, the same trend is not observed for the first eluted enantiomer. Consequently, the second eluted enantiomer has a higher rate constant than the first eluted enantiomer in the strongest proton donor alcohol (MeOH), whereas the converse is true in the weakest alcohol (*t*-BuOH). As the concentration of the modifier increases to 10%, similar trends are observed (Table 7). The desorption rate constant for the first enantiomer increases further in the alcohol modifiers, but decreases in THF. For the second eluted enantiomer, the desorption rate constant increases significantly in MeOH and *i*-BuOH, but decreases in *t*-BuOH and THF. Again, the second eluted enantiomer has a higher rate constant than the first eluted enantiomer in the strong proton donor alcohols (MeOH and *i*-BuOH), whereas the converse is true in the weakest alcohol (*t*-BuOH) and in THF. It may seem somewhat unexpected for the second eluted enantiomer to have a faster desorption rate, since it must necessarily have greater interaction with the chiral selective sites, which are generally thought to be kinetically slower than the achiral sites. However, this behavior has been observed previously for these solutes with β-cyclodextrin stationary phases [32,47].

The desorption rate constants for coumatetralyl enantiomers in varying modifier concentrations are summarized in Table 7 and are compared to values in the absence of modifier in Table 6. At 5% modifier concentration, the desorption rate constants for both enantiomers increase substantially in all modifiers. Again, this behavior is expected for modifiers that serve as better displacing agents than acetonitrile for sites on the derivatized amylose phase. The rate constants are comparable for the first and second eluted enantiomers for most modifiers, but somewhat smaller for the second eluted enantiomer in THF. As the concentration of the modifier increases to 10%, the desorption rate constant for the first eluted enantiomer is found to increase significantly. For the second eluted enantiomer, the desorption rate constant increases significantly in MeOH, *i*-BuOH, and *t*-BuOH, but decreases significantly in THF. In most cases, the rate of mass transfer is faster for the first eluted

Table 7
Effect of organic modifier type and concentration on desorption rate constants (k_{ms}) for warfarin and coumatetralyl enantiomers at 10 °C.

Solute	Modifier	5%		10%	
		$(k_{ms})_1$ [a] (s^{-1})	$(k_{ms})_2$ [a] (s^{-1})	$(k_{ms})_1$ [a] (s^{-1})	$(k_{ms})_2$ [a] (s^{-1})
Warfarin	MeOH	8.3	13.0	14.8	31.1
	i-BuOH	4.5	10.5	10.5	14.2
	t-BuOH	5.7	3.0	11.3	0.6
	THF	7.2	2.5	1.6	1.4
Coumatetralyl	MeOH	1.0	0.8	4.0	2.7
	i-BuOH	1.3	1.0	2.6	2.9
	t-BuOH	0.7	0.6	2.6	0.8
	THF	1.2	0.6	3.2	0.09

[a] Subscripts denote the first (1) and second (2) eluted enantiomers.

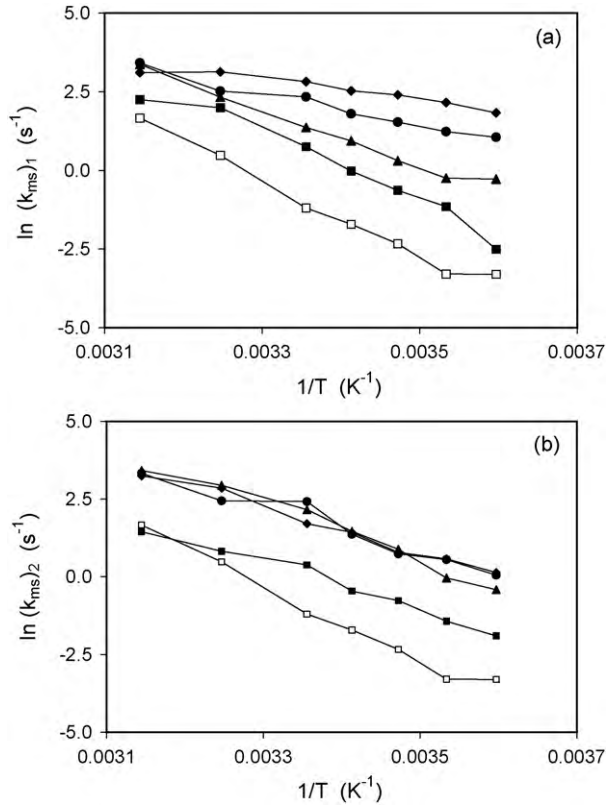

Fig. 9. Arrhenius plots for all coumarin enantiomers: (a) natural logarithm of the desorption rate constant of the first eluted enantiomer (k_{ms1}) versus inverse temperature ($1/T$), (b) natural logarithm of the desorption rate constant of the second eluted enantiomer (k_{ms2}) versus $1/T$. Warfarin (●), coumachlor (▲), coumafuryl (♦), coumatetralyl (■), and 4-hydroxycoumarin (□). Other experimental conditions as given in Fig. 1.

enantiomer than for the second eluted enantiomer, as might be expected.

It is noteworthy that the desorption rate constant for the second eluted enantiomer decreases by 85% as the concentration of THF is increased from 5% to 10%. Consequently, the desorption rate constant for the first eluted enantiomer is about 36 times faster than that for the second eluted enantiomer in 10% THF. This observation may explain why the enantioselectivity of coumatetralyl enantiomers increases from 1.57 to 1.87 in 5% and 10% THF, respectively. Conversely, the desorption rate constant for the second eluted enantiomer increases by 33% as the concentration of *t*-BuOH is increased from 5% to 10%. The enantioselectivity of coumatetralyl enantiomers simultaneously decreases from 1.57 to 1.40. Because the desorption rate constant is inversely related to the retention factor through Eq. (10), it may also exhibit an inverse effect on the enantioselectivity. This effect will only be observed if desorption is the dominant, rate limiting step in the retention mechanism, as demonstrated here for coumatetralyl.

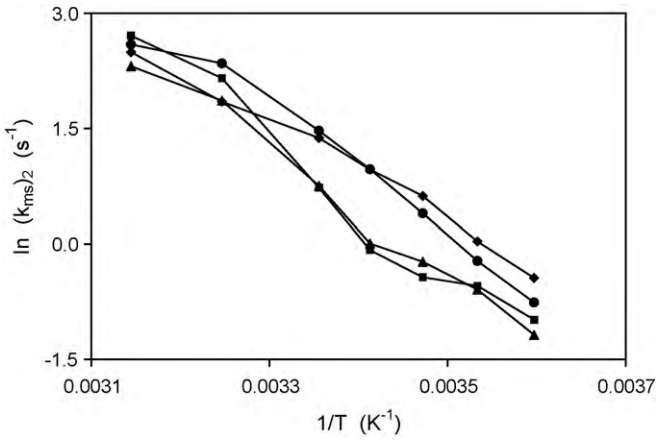

Fig. 10. Arrhenius plots for coumatetralyl: natural logarithm of the desorption rate constant of the second eluted enantiomer (k_{ms2}) versus inverse temperature ($1/T$) in the presence of 5% modifiers. MeOH (●), *i*-BuOH (♦), *t*-BuOH (▲), and THF (■). Other experimental conditions as given in Fig. 1.

3.2.2. Effect of temperature on rate constants

When the solute is transferred between the mobile and stationary phases, it passes through a short-lived, high-energy transition state (‡) that uniquely characterizes the path-dependent aspects of the retention mechanism. The kinetic rate constant is related to the activation energy by means of the Arrhenius equation [41],

$$\ln k_{sm} = \ln A_{\ddagger m} - \frac{\Delta E_{\ddagger m}}{RT} \quad (19)$$

where $A_{\ddagger m}$ is the pre-exponential factor and $\Delta E_{\ddagger m}$ is the activation energy arising from the transition from mobile phase to transition state. The activation energy for the sorption process ($\Delta E_{\ddagger m}$) can be determined from the slope of $\ln k_{sm}$ versus $1/T$, if $A_{\ddagger m}$ and $\Delta E_{\ddagger m}$ are independent of temperature. Likewise, the activation energy for the desorption process ($\Delta E_{\ddagger s}$) can be determined from the slope of $\ln k_{ms}$ versus $1/T$, if $A_{\ddagger s}$ and $\Delta E_{\ddagger s}$ are independent of temperature. When one of these transitions is slow with respect to the mobile phase velocity, it will be manifested chromatographically in the symmetric and asymmetric broadening of the solute zone [35].

The Arrhenius plots for the desorption rate constant ($\ln k_{ms}$ versus $1/T$) of the coumarins in acetonitrile mobile phase are shown in Fig. 9. For both enantiomers, the rate constants increase with an increase in temperature and the plots are relatively linear. Some of the trends observed in Table 6 are evident throughout the temperature range. For the first eluted enantiomer (Fig. 9a), the rate constants for the coumarins are quite diverse. The fastest desorption rate is observed for coumafuryl, while the slowest is for 4-hydroxycoumarin. For the second eluted enantiomer (Fig. 9b), the rate constants for warfarin, coumachlor, and coumafuryl are similar, whereas coumatetralyl and 4-hydroxycoumarin are substantially lower. The slopes of these graphs provide information regarding the activation energy for desorption ($\Delta E_{\ddagger s}$). The activation energies for the first eluted enantiomer are quite diverse,

Table 8
Effect of organic modifier on activation energy of sorption ($\Delta E_{\ddagger m}$) and desorption ($\Delta E_{\ddagger s}$) processes for coumatetralyl enantiomers.

Modifier (5%)	$(\Delta E_{\ddagger m})_1$ [a,b] (kJ/mol)	$(\Delta E_{\ddagger s})_1$ (kJ/mol)	$(\Delta E_{\ddagger m})_2$ [a,b] (kJ/mol)	$(\Delta E_{\ddagger s})_2$ (kJ/mol)
None	70 ± 8	87 ± 8	43 ± 4	63 ± 4
MeOH	50 ± 5	62 ± 5	53 ± 5	65 ± 5
i-BuOH	26 ± 3	35 ± 4	40 ± 3	53 ± 3
t-BuOH	49 ± 2	62 ± 2	51 ± 4	67 ± 4
THF	53 ± 5	68 ± 5	54 ± 7	73 ± 7

[a] Subscripts denote the first (1) and second (2) eluted enantiomers.
[b] Calculated from the slope of Eq. (19).

ranging from 24.5 kJ/mol for coumafuryl to 87.4 kJ/mol for coumatetralyl. In contrast, the activation energies for the second eluted enantiomer are more similar, ranging from 60.2 kJ/mol for coumafuryl to 62.6 kJ/mol for coumatetralyl. The achiral solute, 4-hydroxycoumarin, has a much higher activation energy of 96.9 kJ/mol.

The effect of organic modifiers is demonstrated in the representative Arrhenius plot for the coumatetralyl enantiomers in Fig. 10, together with corresponding values for the activation energy in Table 8. In all modifiers, the activation energy for sorption is lower than that for desorption for both coumatetralyl enantiomers. However, because of the uncertainty in these measurements, both enantiomers have statistically equivalent activation energies for sorption and, similarly, have statistically equivalent activation energies for desorption. Moreover, with the exception of *i*-BuOH, the activation energies for sorption are comparable in all modifiers and, similarly, the activation energies for desorption are comparable in all modifiers. Although the activation energies are comparable, the desorption rate constants differ significantly, especially for the second eluted enantiomer of coumatetralyl (Table 7). This suggests that the pre-exponential factor in Eq. (19), which is related to the activation entropy for desorption ($\Delta S_{\ddagger s}$), may play an important role in governing the kinetic behavior. This behavior has been observed previously for the coumarin solutes on β-cyclodextrin stationary phases [32].

4. Conclusions

In this paper, the effect of temperature and organic modifiers on the enantioseparation of coumarin-based solutes on Chiralpak IA stationary phase is examined. Thermodynamic values in acetonitrile mobile phase indicate that coumatetralyl enantiomers have the most favorable changes in molar enthalpy, whereas warfarin, coumachlor, and coumafuryl have smaller, more comparable values. The changes in molar enthalpy vary with organic modifier, where values in the presence of MeOH and *i*-BuOH are smaller than those in *t*-BuOH and THF for both warfarin and coumatetralyl. In general, retention and enantioselectivity decrease as concentration and proton donating ability of the alcohol modifiers increases. On the other hand, retention and enantioselectivity remain constant or increase as concentration of the proton acceptor THF increases.

Temperature also influences the thermodynamics and kinetics of the separation. In general, retention and enantioselectivity of the coumarins decrease as the temperature increases. The van't Hoff plots show linear behavior for small modifiers (such as MeOH) at low concentration, as well as non-linear behavior for bulky modifiers (such as *t*-BuOH and THF). The non-linear plots are attributed to conformational changes in the stationary phase and are observed around room temperature (20–25 °C). Enthalpy–entropy compensation plots suggest that the retention mechanism of all coumarin solutes may be similar in acetonitrile mobile phase. On the other hand, compensation is not observed for warfarin and coumatetralyl enantiomers separated in the presence of organic modifiers. This suggests that the retention mechanism of the individual enantiomers is distinctly different in each modifier. Overall, the first eluted enantiomers show no discernable enthalpy–entropy compensation, whereas the second eluted enantiomers show nearly linear compensation in each modifier. Because the second enantiomer interacts more strongly with the chiral selective sites of the derivatized amylose phase, this may imply that the chiral sites have a more similar retention mechanism than the achiral sites in each organic modifier.

The kinetic data demonstrate that the sorption rate is always faster than the desorption rate for all coumarin solutes and for all mobile phase compositions. An increase in the concentration of alcohol modifiers causes an increase in the desorption rate. This suggests that the alcohols are serving as displacing or competing agents for the adsorption sites in the derivatized amylose phase. In contrast, the desorption rate decreases as the concentration of THF increases. This effect is most pronounced for the second eluted enantiomer of coumatetralyl, for which the desorption rate constant is 36 times slower than the first eluted enantiomer, leading to a substantial increase in enantioselectivity. These thermodynamic and kinetic data provide detailed insight into the mechanism of chiral separations on Chiralpak IA.

Acknowledgements

The authors gratefully acknowledge Dr. Geoffrey B. Cox (Chiral Technologies Inc.) for providing the tris-(3,5-dimethylphenyl carbamate) derivatized amylose stationary phase (Chiralpak IA) and for helpful discussions.

References

[1] Y. Okamoto, M. Kawashima, K. Yamamoto, K. Hatada, Chem. Lett. (1984) 739.
[2] Y. Okamoto, R. Aburatani, T. Fukumoto, K. Hatada, Chem. Lett. (1987) 1857.
[3] Y. Okamoto, M. Kawashima, K. Hatada, J. Am. Chem. Soc. 106 (1984) 5357.
[4] K.G. Lynam, R.W. Stringham, Chirality 18 (2006) 1.
[5] D. Mangelings, M. Maftouh, Y. Vander Heyden, J. Sep. Sci. 28 (2005) 691.
[6] Y. Okamoto, Y. Kaida, J. Chromatogr. A 666 (1994) 403.
[7] Y. Okamoto, E. Yashima, Angew. Chem. Int. Ed. 37 (1998) 1020.
[8] E. Yashima, J. Chromatogr. A 906 (2001) 105.
[9] E. Yashima, Y. Okamoto, Bull. Chem. Soc. Jpn. 68 (1995) 3289.
[10] T. Zhang, C. Kientzy, P. Franco, A. Ohnishi, Y. Kagamihara, H. Kurosawa, J. Chromatogr. A 1075 (2005) 65.
[11] J.E. Schiel, D.S. Hage, J. Sep. Sci. 32 (2009) 1507.
[12] M. Lammerhofer, J. Chromatogr. A 1217 (2010) 814.
[13] W.H. Pirkle, J. Chromatogr. 558 (1991) 1.
[14] T.D. Booth, I.W. Wainer, J. Chromatogr. A 741 (1996) 205.
[15] Y.F. Ming, L. Zhao, H.L. Zhang, Y.P. Shi, Y.M. Li, Chromatographia 64 (2006) 273.
[16] R.J. Smith, D.R. Taylor, S.M. Wilkins, J. Chromatogr. A 697 (1995) 591.
[17] W. Weng, H.X. Guo, F.P. Zhan, H.L. Fang, Q.X. Wang, B.X. Yao, S.X. Li, J. Chromatogr. A 1210 (2008) 178.
[18] F. Wang, D. Yeung, J. Han, D. Semin, J.S. McElvain, J. Cheetham, J. Sep. Sci. 31 (2008) 604.
[19] R. Cirilli, M.R. Del Giudice, R. Ferretti, F. La Torre, J. Chromatogr. A 923 (2001) 27.
[20] M. Kazusaki, H. Kawabata, H. Matsukura, J. Liq. Chromatogr. Rel. Technol. 23 (2000) 2937.
[21] T. O'Brien, L. Crocker, R. Thompson, K. Thompson, P.H. Toma, D.A. Conlon, B. Feibush, C. Moeder, G. Bicker, N. Grinberg, Anal. Chem. 69 (1997) 1999.
[22] F. Wang, T. O'Brien, T. Dowling, G. Bicker, J. Wyvratt, J. Chromatogr. A 958 (2002) 69.
[23] A.M. Rizzi, J. Chromatogr. 478 (1989) 71.
[24] R.M. Wenslow, T. Wang, Anal. Chem. 73 (2001) 4190.
[25] F. Wang, R.M. Wenslow, T.M. Dowling, K.T. Mueller, I. Santos, J.M. Wyvratt, Anal. Chem. 75 (2003) 5877.
[26] R.B. Kasat, Y. Zvinevich, H.W. Hillhouse, K.T. Thomson, N.H.L. Wang, E.I. Franses, J. Phys. Chem. B 110 (2006) 14114.
[27] S.C. Chang, I.G. Reid, S. Chen, C.D. Chang, D.W. Armstrong, Trends Anal. Chem. 12 (1993) 144.
[28] B. Chankvetadze, I. Kartozia, C. Yamamoto, Y. Okamoto, J. Pharm. Biomed. Anal. 27 (2002) 467.
[29] K.G. Gebreyohannes, V.L. McGuffin, J. Liq. Chromatogr. Rel. Technol., submitted for publication.
[30] J.C. Gluckman, A. Hirose, V.L. McGuffin, M. Novotny, Chromatographia 17 (1983) 303.
[31] S.B. Howerton, C. Lee, V.L. McGuffin, Anal. Chim. Acta 478 (2003) 99.
[32] X.P. Li, V.L. McGuffin, J. Liq. Chromatogr. Rel. Technol. 30 (2007) 965.
[33] V.L. McGuffin, C.E. Evans, J. Microcolumn Sep. 3 (1991) 513.
[34] X. Li, A.M. Hupp, V.L. McGuffin, in: E. Grushka, N. Grinberg (Eds.), Advances in Chromatography, CRC Press, Boca Raton, FL, 2007.
[35] J.C. Giddings, Dynamics of Chromatography, Part I: Principles and Theory, Dekker, Inc., NY, 1965.
[36] J.J. Vandeemter, F.J. Zuiderweg, A. Klinkenberg, Chem. Eng. Sci. 5 (1956) 271.
[37] A.M. Hupp, V.L. McGuffin, J. Liq. Chromatogr. Rel. Technol., in press.
[38] M.J. Kamlet, J.L.M. Abboud, M.H. Abraham, R.W. Taft, J. Org. Chem. 48 (1983) 2877.

[39] M.J. Gidley, S.M. Bociek, J. Am. Chem. Soc. 110 (1988) 3820.
[40] T. Wang, R.M. Wenslow, J. Chromatogr. A 1015 (2003) 99.
[41] P.W. Atkins, Physical Chemistry, 6th ed., W.H. Freeman, New York, 1987.
[42] I. Spanik, J. Krupcik, V. Schurig, J. Chromatogr. A 843 (1999) 123.
[43] R.R. Krug, W.G. Hunter, R.A. Grieger, J. Phys. Chem. 80 (1976) 2335.
[44] R.R. Krug, W.G. Hunter, R.A. Grieger, J. Phys. Chem. 80 (1976) 2341.
[45] J.J. Li, P.W. Carr, J. Chromatogr. A 670 (1994) 105.
[46] B.X. Yao, F.P. Zhan, G.Y. Yu, Z.F. Chen, W.J. Fan, X.P. Zeng, Q.L. Zeng, W. Weng, J. Chromatogr. A 1216 (2009) 5429.
[47] X. Li, V.L. McGuffin, J. Liq. Chromatogr. Rel. Technol. 30 (2007) 937.